Nosaka, Y. Finite depth spherical well model for excited states of ultrasmall semiconductor particles: an application. J. Phys. Chem. 95, 5054-5058

ARTICLE *in* THE JOURNAL OF PHYSICAL CHEMISTRY · JUNE 1991

Impact Factor: 2.78 · DOI: 10.1021/j100166a028

1 AUTHOR:

Yoshio Nosaka
Nagaoka University of Technology
228 PUBLICATIONS **5,741** CITATIONS

SEE PROFILE

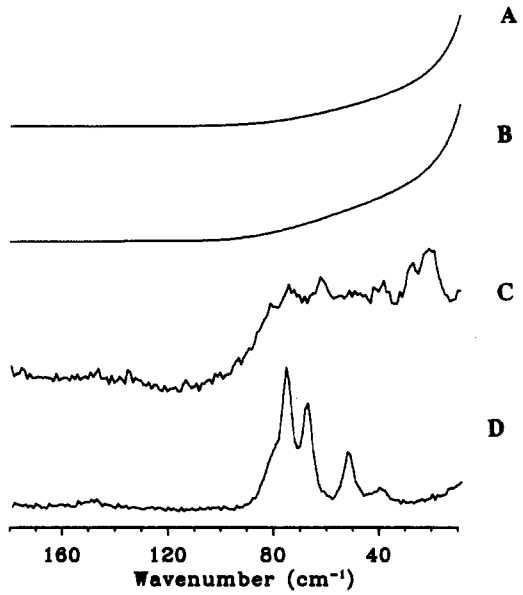

Figure 4. Raman spectra of the low-frequency region of cyclooctane: (A) 235 K (phase I); (B) 170 K (phase II); (C) 60 K (phase III'); (D) 55 K (phase III).

Several other monocyclic compounds have been shown to form a glassy phase on rapid cooling[10] in which the nature of the metastable phases can be related to their corresponding disordered phases. In such cases, the low-frequency lattice region in the Raman spectrum usually exhibits a broad weak band. In phase III' of cyclooctane, at least five very weak external modes were observed in the lattice region, Figure 4, superimposed upon a broad peak. The nature of phase III' is, therefore, not that of a glassy crystal, since it must be at least partly ordered, but may involve multiple conformers frozen-in from phase I but with pseudorotation still persisting.

The ring deformation modes are particularly sensitive indicators of pseudorotation and conformational changes. The boat-chair conformation should have six symmetric and four antisymmetric ring-bending vibrations. In disordered phase I, nine of the ten expected modes were observed and only the lowest energy band was missing. The bands were broad and very close in frequency to the values found for the liquid, indicating the presence of significant molecular motion. In phase III, the lowest energy mode appeared at 150 cm^{-1}, and all the bands were sharp. As expected, the degree of molecular motion is drastically reduced in the ordered phase. Quite large shifts in frequency were observed, for example, bands at 213 and 246 cm^{-1} in phase I shifted by 11 and 13 cm^{-1}, respectively, to 224 and 259 cm^{-1} phase III at 55 K. The same bands occupied intermediate positions in phase III'. These large shifts at the phase transitions are typical of these monocyclic compounds[10,14-16] and arise from the increased intermolecular forces in the higher density, closer packed ordered phase.

In summary, the vibrational spectra of solid cyclooctane have been measured and the sequence of transitions can be followed quite clearly from the changes in the vibrational spectra as a function of temperature. The lowest temperature phase is the only ordered phase, with either C_2 or C_s symmetry with two molecules per unit cell. The existence of the metastable phase has been confirmed. This phase has a different space group from any of the other phases and is not a glassy crystal.

Acknowledgment. This research was supported by operating and equipment grants from NSERC (Canada) and FCAR (Quebec). Y.H. gratefully acknowledges the award of a graduate fellowship from McGill University.

Registry No. Cyclooctane, 292-64-8.

(14) Haines, J.; Gilson, D. F. R. *Can. J. Chem.* **1989**, *67*, 941.
(15) Haines, J.; Gilson, D. F. R. *J. Phys. Chem.* **1989**, *93*, 6237.
(16) Haines, J.; Gilson, D. F. R. *J. Chem. Soc., Faraday Trans.* **1990**, *86*, 2617.

Finite Depth Spherical Well Model for Excited States of Ultrasmall Semiconductor Particles. An Application

Yoshio Nosaka

Department of Chemistry, Nagaoka University of Technology, Kamitomioka, Nagaoka, 940-21 Japan
(Received: September 12, 1990; In Final Form: February 11, 1991)

A formula to calculate the energy level with a finite depth potential well model is proposed. Coulomb interaction energy of the electron–hole pair was estimated with this model. The excitation energy of an ultrasmall CdS particle was comparable with literature values. The present calculation of excitation energy is easily adoptable to any semiconductor particle. A virtual leakage of the conduction band electron outside the semiconductor sphere is found to be proportional to the experimentally obtained rate of photoinduced surface electron transfer.

Introduction

Ultrasmall semiconductor particles with diameters of the order of nanometers have been paid special attention because of their unique size-dependent properties, which include optical properties such as absorption spectra and third-order nonlinearity as well as physicochemical properties.[2] Since the size dependence of the band levels of semiconductor particles results in a shift of optical spectrum, quantum mechanical descriptions of the shift were carried out by several researchers.[3-14] Efros and Efros[3] simply assumed a spherically symmetric well with infinitely high wall and ignored the Coulomb interaction between an electron and a

(1) Steigerwald, M. L.; Brus, L. E. *Acc. Chem. Res.* **1990**, *23*, 183.
(2) Henglein, A. *Chem. Rev.* **1989**, *89*, 1861.
(3) Efros, Al.L.; Efros, A. L. *Sov. Phys., Semicond.* **1982**, *16*, 772.
(4) Brus, L. E. *J. Chem. Phys.* **1983**, *79*, 5566.
(5) Brus, L. E. *J. Chem. Phys.* **1984**, *80*, 4403.
(6) Rossetti, R.; Ellison, J. L.; Gibson, J. M.; Brus, L. E. *J. Chem. Phys.* **1984**, *80*, 4464.
(7) Fojtik, A.; Weller, H.; Koch, U.; Henglein, A. *Ber. Bunsen-Ges. Phys. Chem.* **1984**, *88*, 969.
(8) Weller, H.; Schmidt, H. M.; Koch, U.; Fojtik, A.; Baral, S.; Henglein, A.; Kunath, W.; Weiss, K.; Dieman, E. *Chem. Phys. Lett.* **1986**, *124*, 557.
(9) Schmidt, H. M.; Weller, H. *Chem. Phys. Lett.* **1986**, *129*, 615.
(10) Kayanuma, Y. *Solid State Commun.* **1986**, *59*, 405; *Phys. Rev. B* **1988**, *38*, 9797.
(11) Nair, S. V.; Sinha, S.; Rustagi, K. C. *Phys. Rev. B* **1987**, *35*, 4098.
(12) Rajh, T.; Peterson, M. W.; Turner, J. A.; Nozik, A. J. *J. Electroanal. Chem.* **1987**, *228*, 55.

0022-3654/91/2095-5054$02.50/0

hole. Brus[5,6] evaluated the energies including Coulomb interaction and polarization of the lowest state by using a confined exciton model, in which the eigenfunction is equivalent to that obtained for the infinite depth well. This report[5] showed that the Coulomb interaction energy between an electron and a hole in the semiconductor sphere was not small enough to be neglected. Weller et al.[8] modified a wave function to account for the Coulomb interaction. Schmidt and Weller[9] used a Hylleraas-type function and compared it with other eigenfunctions. A similar variational calculation for the confined exciton was also reported.[10,11] In the confined exciton models, the infinite depth well has usually been assumed. Brus[4] applied first the finite depth well model to the excited state of ultrasmall semiconductor particles. Henglein and co-workers[8] compared the calculation methods based on the experimental observations for CdS and showed that a realistic assumption of a finite potential energy step at the crystalline surface improves the model considerably. Since the report did not describe the details of the calculation, similar calculations for other semiconductors cannot be easily performed. Although Nozik and co-workers[12] used a finite depth well, the Coulomb interaction has been ignored, and the results could not easily be applied to other semiconductors.

In this report we will focus on the finite depth potential well model[4] to take into account the real finite energy step at the particle surface. At first, an easy method is proposed to estimate the size dependence of energy levels for any semiconductor whose conduction band level and effective mass of carriers are known. The obtained results appear to agree with those of a more sophisticated theory. The Coulomb interaction energy will be calculated numerically by using the eigenfunction for the finite depth well. Although leakage of electrons outside the particle results from the present model, it will be shown that the amount of the leakage relates to the experimental data for the rate of photoinduced surface electron transfer.

Results and Discussion

Kinetic Energy. On the conventional infinite depth well model, excitation energy level E_{ln} of an ultrasmall semiconductor particle with radius R can be expressed by the bandgap energy E_g of bulk semiconductor and kinetic energy. In a simple way, the kinetic energy can be calculated as the energy of a particle in a box having a spherically symmetric square well potential of infinite depth.[3]

$$E_{ln} = E_g + (\hbar^2/2\mu R^2)\phi_{ln}^2 \qquad (1)$$

where μ is the reduced effective mass of the conduction band electron and valence band hole, which are represented hereafter by m_e^* and m_h^*, respectively. ϕ_{ln} is the nth root of the spherical Bessel function of lth order. For the lowest 1s excited state, $\phi_{01} = \pi$.

When the depth of the potential well is finite, no analytical formula was obtained.[15] Although the solving method has been described for some low energy levels,[15] a general presentation of energy calculation has not been described. In the present study, the energy levels are calculated numerically by formulating the equations as shown in the Appendix. The effective mass m^* is used only inside the well, although Rajh et al.[12] used m^* even outside the semiconductor sphere. In the boundary condition at the surface, derivatives of the wave function were divided by the mass. This condition, which has been already adopted by Brus,[4] is based on the continuation of charge flux crossing at tunnel injections.[16]

The calculation was performed with a personal computer. Figure 1 shows the energy levels and eigenfunctions of conduction band electron of CdS for three different radii. The arrows in the figure indicate the energy levels obtained for the infinite potential depth, i.e., $V_0 = \infty$. Eigenfunctions in Figure 1 show the penetration of the electron into the wall, indicating the electron leaks from the particle. We will discuss the leakage in the last section.

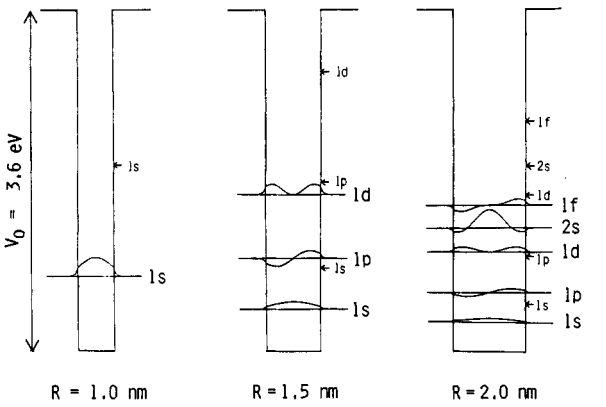

Figure 1. Energy levels and eigenfunctions of particles having effective mass of $0.19m_e$ in the finite depth (V_0 = 3.6 eV) spherical well. See the Appendix for the calculation method. Arrows show the energy levels for $V_0 = \infty$.

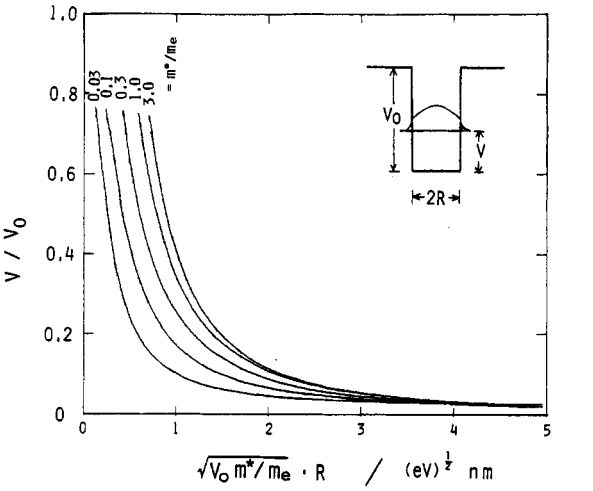

Figure 2. Relative energy level V/V_0 of the 1s state of semiconductor particles characterized by potential depth V_0, effective mass m^*, and radius R.

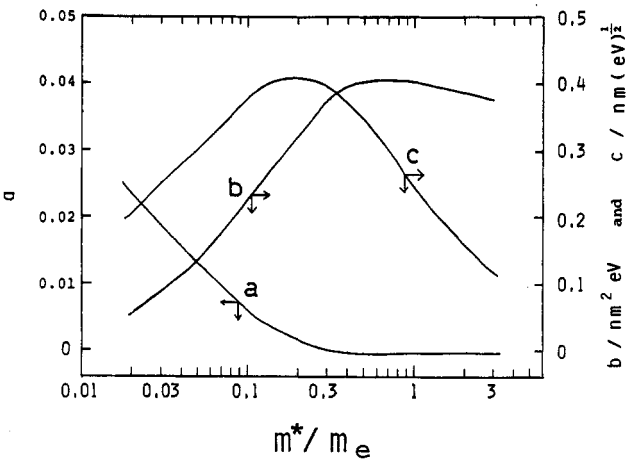

Figure 3. Parameters for eq 2 as a function of effective mass m^*.

It seems useful if we can obtain easily the lowest excitation energy for any semiconductor which is characterized with V_0 and m^*. Figure 2 shows a collective result obtained for the 1s state by numerical calculation. In this plot, the curves do not diverge much for a change in m^* 2 orders of magnitude. The curve for each m^* can be approximately described by the following equation

$$V/V_0 = a + b/\{(V_0 m^*/m_e)^{1/2}R + c\}^2 \qquad (2)$$

where a, b, and c are the parameters whose values can be read from Figure 3 for a given m^*.

(13) Wang, Y.; Suna, A.; Mahler, W.; Kasowski, R. *J. Chem. Phys.* **1987**, *87*, 7315.
(14) Lippens, P. E.; Lannoo, M. *Phys. Rev. B* **1989**, *39*, 10935.
(15) Schiff, L. I. *Quantum Mechanics*, 3rd ed.; McGraw-Hill: New York, 1968; p 83.
(16) Ben Daniel, D. J.; Duke, C. B. *Phys. Rev.* **1966**, *152*, 683.

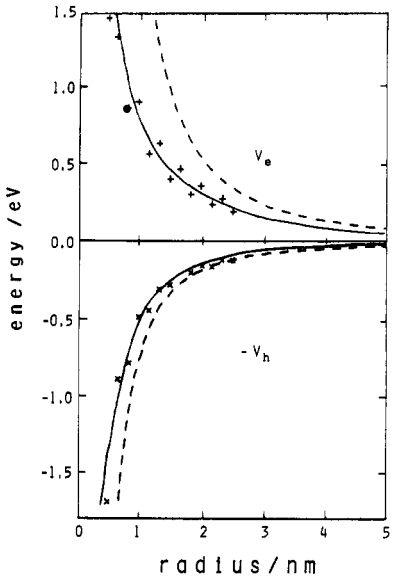

Figure 4. Energy shift for conduction band electron V_e and valence band hole V_h calculated for $m_e^* = 0.18m_e$ and $m_h^* = 0.53m_e$, respectively. Solid curve, $V_0 = 3.6$; dashed curve, $V_0 = \infty$. + and × are the results of tight-binding theory by Lippens and Lannoo.[14]

An example of a useful application of Figure 2 is the estimation of reduced mass. Persans et al.[17] measured the optical spectrum and X-ray diffraction pattern for CdSe-doped filter glass and obtained $V = 0.12$ eV and $R = 2.9$ nm, respectively. They discussed a large value of the effective mass ($m^* = 0.38m_e$) estimated from the infinite depth well model. The infinite depth was regarded as one of the possible reasons for the large value of m^*. By using Figures 2 and 3, it is calculated easily that $m^* = 0.28m_e$ even if $V_0 = 3.0$ eV. Thus, other reasons are mainly responsible for the large m^*.

The energy V can be calculated by using eq 2 for both the conduction band electron and valence band hole, which corresponds to the shift of the band energies with decreasing the radius. The shift of the conduction band energy V_e and the valence band energy V_h for CdS are calculated with m_e^* and m_h^*, respectively, and both are plotted in Figure 4 as a function of radius. The result of tight-binding theory reported by Lippens and Lannoo,[14] which is replotted in the figure, agrees well with the result of a simple calculation on the present model.

The kinetic energy of the excited state is the sum of the both energy values, $V_e + V_h$.

Coulomb Interaction Energy. Energy for the Coulomb interaction between an electron and a hole in a semiconductor can be evaluated numerically by using the eigenfunction obtained by the spherical quantum well calculation. The formula used in the evaluation is shown in the Appendix. The Coulomb energy for 1s–1s state of an electron–hole pair was calculated for CdS and plotted in Figure 5 as a function of radius. The kinetic energy is also plotted in Figure 5, where $m_e^* = 0.19m_e$ and $m_h^* = 0.80m_e$. Figure 5 also shows energies for the infinite depths of potential. While a significant difference between finite and infinite depths was observed in the curves of kinetic energy, the difference for Coulomb energy is rather small.

Brus et al.[5] showed that the Coulomb interaction energy E_c can be calculated by eq 3 where $C_1 = 1.8$.

$$E_c = -C_1 e^2/\epsilon R \qquad (3)$$

This expression was supported by Kayanuma[10] and Schmidt and Weller[9] with $C_1 = 1.786$. The value of C_1 was obtained analytically by using an eigenfunction for the infinite depth well. Then this equation can be used for approximate estimation of the Coulomb energy on the finite depth well model.

(17) Persans, P. D.; An, T.; Wu, Y.-J.; Lewis, M. *J. Opt. Soc. Am. B* **1989**, *6*, 818.

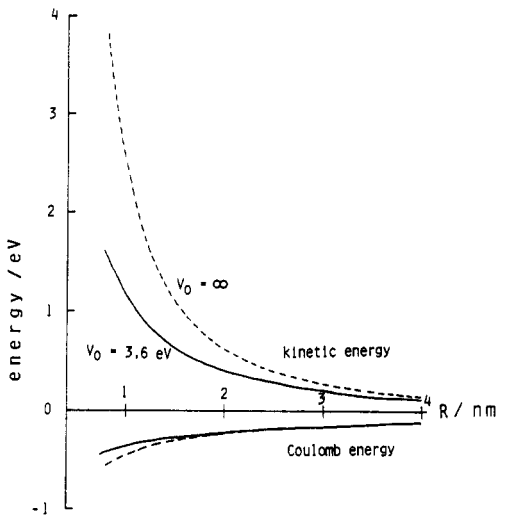

Figure 5. Kinetic and Coulomb energies calculated for ultrasmall CdS particles. $m_e^* = 0.19m_e$, $m_h^* = 0.80m_e$, and $\epsilon = 5.6$.

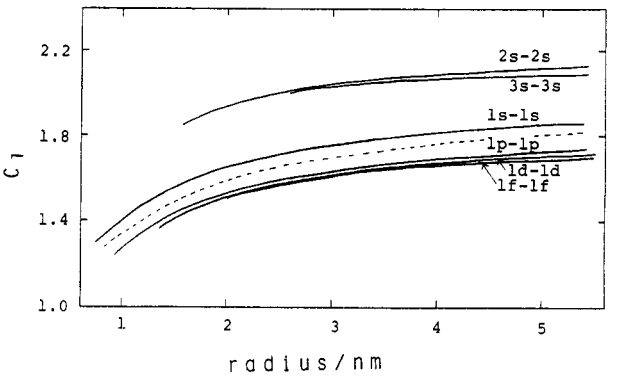

Figure 6. Parameter C_1 in eq 3 deduced from the Coulomb energy calculated with the wave functions for $m_e^* = 0.19m_e$, $m_h^* = 0.80\ m_e$, and $V_0 = 3.6$ eV. The dashed curve is for the 1s–1s Coulomb energy for effective masses of $m_e^* = 0.18m_e$ and $m_h^* = 0.53m_e$.

In order to show conspicuously the effect of the finite depth potential, eq 3 was adopted reversally to calculate C_1 from E_c. Values of C_1 thus calculated depend on the radius as shown in Figure 6. The dashed curve in the figure shows that C_1 depends on m^* as well. For 1p–1p state of the electron–hole pair, the value of C_1 is smaller than that for the 1s–1s state at every R. Since the electron–hole distance for the 1p–1p state may be larger than that for the 1s–1s state, the Coulomb energy of the 1p–1p state is presumably smaller. Although the values of 1.889[9] and 1.884[10] were reported on the confined exciton model with $V_0 = \infty$, the present result seems reasonable. It was confirmed by separate calculations that, when V_0 increases, the values of C_1 for 1s–1s and 1p–1p are close to the constants cited above, respectively.

Excitation Energy. When the values of E_g, m_e^*, m_h^*, ϵ, and V_0 are known, excitation energy E_{ex} of ultrasmall semiconductor particles is given by the following equation

$$E_{ex} = E_g + V_e + V_h + E_c \qquad (4)$$

where V_e and V_h can be calculated by eq 2 with m_e^* and m_h^* for the lowest state, and E_c can be obtained by eq 3 with the constant C_1 in a good accuracy.

For ultrasmall CdS particles, the present result can be compared with that in the literature. In Figure 7, the excitation energy in the scale of wavelength is plotted as a function of diameter. The curves taken from the reports were calibrated to $E_g = 2.4$ eV. Curve a in the figure was calculated by eq 1. Curve b was improved by the Coulomb interaction and is comparable with the results of confined exciton calculation reported by Brus[5] and Schmidt and Weller.[9] The former result contains the polarization effect and the latter was obtained by using a Hylleraas-type function. Curve c was obtained for the finite depth well with eq

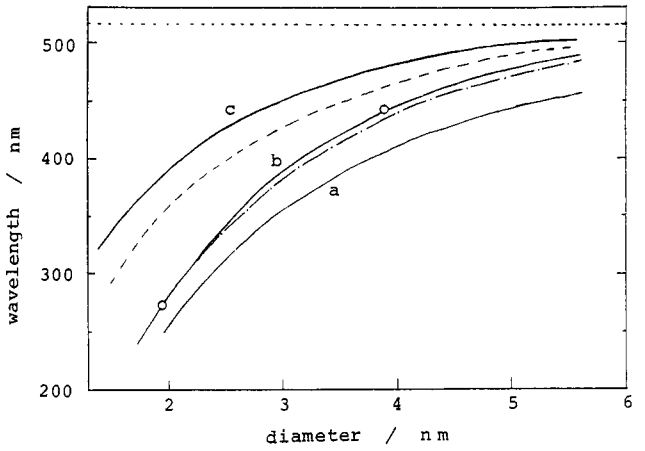

Figure 7. Comparison of the calculated lowest excitation energies for CdS particles. Curve a corresponds to eq 1 ($V_0 = \infty$); Curves b and c are calculated by eq 4 with $V_0 = \infty$ and 3.6 eV, respectively. The dashed curve,[8] dashed-dotted curve,[5] and open circles[9] are obtained from the literature. The dotted line (λ = 516 nm) corresponds to E_g of 2.4 eV.

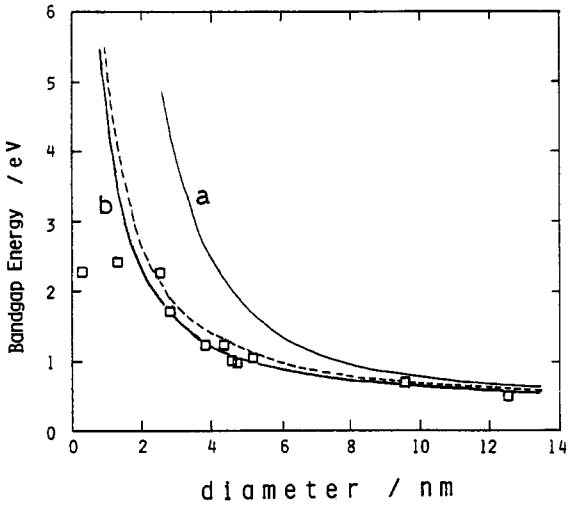

Figure 8. Bandgap energy of PbS ultrasmall particles calculated with the present model for $V_0 = \infty$ (a) and 4.5 eV (b). $m_e^* = m_h^* = 0.085m_e$, E_g = 0.41 eV, and ϵ = 17.2. The dashed curve is the calculated result based on the hyperbolic band model, and □ are experimental data; both were reported by Wang et al.[13]

4. On comparing curves a–c, the finite depth effect becomes larger than the Coulomb interaction energy at diameters less than 4 nm. If the polarization term[5] is taken into consideration, curve c closes to the dashed curve which is recommended from experimental results.[8]

Wang et al.[13] claimed that the electron–hole in a box model with effective mass approximation cannot explain the size dependence of the energy level of PbS. They proposed a hyperbolic band model to include band nonparabolicity. By adopting the same effective mass ($m_e^* = m_h^* = 0.085m_e$) and V_0 = 4.5 eV, however, the energy calculated with the present model agrees well with the experimental data in the report as shown in Figure 8. This agreement, however, does not prove that the effective mass physical assumption is correct for PbS, because the bands are not parabolic in the bulk material.

Virtual Leakage of Electron. One of the differences between the finite depth well model and the infinite depth one is the penetration of the electron to the potential wall, or leakage outside the particle, associated with the decrease of the kinetic energy as shown in Figure 1. The effective mass corresponds reciprocally to the curvature of the quadratic relation of the momentum to the kinetic energy of electrons in semiconductor.[18] This means that, if the quadratic relation remains at small particle, the decrease of kinetic energy corresponds to the increase of the effective mass. The other way around, by assuming that the effective mass is constant in a small particle, the quadratic relation of the band may be broken; i.e., the leakage corresponds to the increase of the effective mass, which cannot be introduced in the infinite well model.

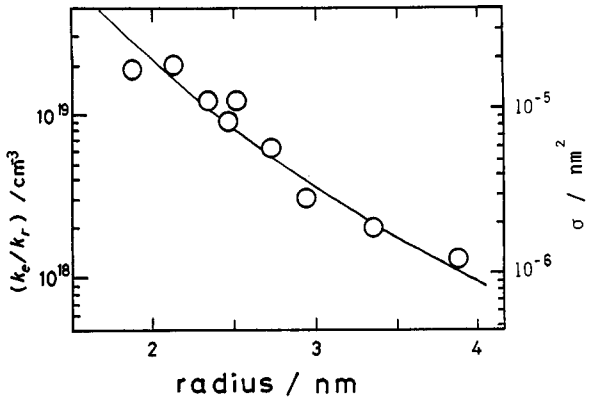

Figure 9. Comparison of the surface excited-electron density (σ) calculated from the finite depth well model and the ratio of reaction rates (k_e/k_r) of electron transfer and electron–hole recombination obtained experimentally.[19]

The amount of leakage for the conduction band electron can be calculated by integrating $\Psi(r)^2$ with respect to r from R to ∞. In Figure 9 the amount per unit surface area, which may be regarded as surface electron density σ, is plotted as a function of R. The open circle is the experimental result[19] for the ratio of rate constant of photoinduced surface electron transfer (k_e) to that of electron–hole recombination (k_r). Since the dependence of k_r on the radius is probably small,[19] Figure 9 indicates that k_e is proportional to σ. If the electron of the excited state actually leaks outside the semiconductor, the result may be easily understood. The correct understanding about the eigenfunctions of the well model is to be an envelope function for the Wannier functions of the energy band in the semiconductor,[20] meaning that the leakage of electron is virtual. From this viewpoint, the electron-transfer rate is explained to be proportional to the magnitude of the Wannier function at the outermost unit lattice of the microcrystalline. However, further theoretical analysis may need experimental data about the real microcrystalline surface.

Conclusion

We showed the method to calculate the excitation energy of ultrasmall semiconductor particles by modeling the finite depth spherically symmetric square quantum well.[4] A numerical formula is proposed to calculate the kinetic energy, on the basis of the band level and effective mass of the bulk semiconductor. The Coulomb interaction energy of the electron–hole pair in the finite depth well model depends on the effective mass as well as radius. But, it was not much different from that calculated for the infinite depth model. The energies of higher excited states, calculated by the present method, may be used to simulate the absorption spectra.[21] In the finite depth well model, the leakage of electrons outside the particle at a small diameter can be regarded as the increase of the effective mass. By comparison with experimental data, the photoinduced electron-transfer rate at CdS surface was shown to be proportional to the amount of the leakage.

Acknowledgment. This study is partly supported by Grant-in-Aids for Scientific Research (No. 01603517, 02203221) from the Ministry of Science, Education and Culture.

Appendix

General Solution for the Finite Depth Well Model. The Schroedinger equation for the spherically symmetric square well potential is written as[4,15]

(18) Kittel, C. *Introduction to Solid State Physics*, 6th ed.; John Wiley: New York, 1986; p 193.

(19) Nosaka, Y.; Ohta, N.; Miyama, H. *J. Phys. Chem.* **1990**, *94*, 3752.
(20) Hanamura, E. *Phys. Rev. B* **1988**, *37*, 1273.
(21) Nosaka, Y.; Ohta, N.; Miyama, H. *Denki Kagaku* **1989**, *57*, 1163.

$$(\hbar^2/2m)\{\nabla^2 + U(r) - E\}\Psi(r)Y_l(\theta,\phi) = 0 \quad \text{(A1)}$$

with

$$U(r) = -V_0 \quad \text{and} \quad m = m^*, \quad \text{at } r < R$$

$$U(r) = 0 \quad \text{and} \quad m = m_e, \quad \text{at } r \geq R$$

where $Y_l(\theta,\phi)$ is the spherical harmonics, V_0 is depth of the well, m^* represents effective mass, and m_e is the mass of electron. V_0 corresponds probably to the difference between the conduction band level of the semiconductor and the adiabatic electron affinity of the medium. The radial part of the eigenfunction is

$$\Psi(r) = Aj_l(\alpha r) \quad \text{at } r < R \quad \text{(A2)}$$

$$\Psi(r) = Bh_l^{(1)}(i\beta r) \quad \text{at } r \geq R \quad \text{(A3)}$$

where $j_l(\alpha r)$ is the spherical Bessel function of lth order and $h_l^{(1)}(i\beta r)$ is the spherical Hankel function of the first kind, and

$$\alpha = \{2m^*(V_0 - E)\}^{1/2}/\hbar \quad \text{(A4)}$$

$$\beta = \{2m_eE\}^{1/2}/\hbar \quad \text{(A5)}$$

The energy levels are obtained by requiring smooth connection at $r = R$. That is equivalent to the following two conditions[4]

$$Aj_l(\alpha R) = Bh_l^{(1)}(i\beta R) \quad \text{(A6)}$$

$$(A/m^*)|\partial j_l(\alpha r)/\partial r|_{r=R} = (B/m_e)|\partial h_l^{(1)}(i\beta r)/\partial r|_{r=R} \quad \text{(A7)}$$

These equations for $l = 0$ and 1 may be solved by analyzing the function.[15] For higher l, however, this method is not convenient. To solve numerically these equations the asymptotic expression for the Bessel functions can be used. The general eigenvalue can be obtained by the following real function.

$$F_l(\xi,\eta) = \xi j_{l-1}(\xi)h_l(\eta) + (l+1)(m^*/m_e - 1)j_l(\xi)h_l(\eta) + (m^*/m_e)\eta j_l(\xi)h_{l-1}(\eta) \quad \text{(A8)}$$

for $l \geq 1$, and

$$F_0(\xi,\eta) = (\xi/\tan\xi) + (m^*/m_e - 1) + (m^*/m_e)\eta \quad \text{(A9)}$$

where

$$\xi = \alpha R, \quad \eta = \beta R$$

$$h_l(\eta) = h_l^{(1)}(i\eta)(i)^{l-2}\exp(\eta) \quad \text{(A10)}$$

The value of E which brings $F_l(\xi,\eta) = 0$ for a given R is an eigenvalue of the Schroedinger equation (eq A1). For numerical solving, the first derivative of $F_l(\xi,\eta)$ with respect to E was formulated analytically.

The eigenfunction $\Psi(r)$ can be calculated from eqs A2-A6 for each E obtained. The energy level V measured from the bottom of the well is given by $V = V_0 - E$.

Coulomb Interaction Energy. Energy of Coulomb interaction between electron and hole in a spherical semiconductor quantum well may be calculated as

$$E_c = -(e^2/\epsilon)\int_0^\infty\int_0^\infty\int_0^\pi (r^2 + r_h^2 - 2rr_h\cos\theta)^{-1/2}\{\Psi(r)\Psi_h(r_h)rr_h\}^2 \sin\theta\, d\theta\, dr\, dr_h \quad \text{(A11)}$$

where e is the elementary charge, ϵ represents the dielectric constant of the semiconductor, and $\Psi(r)$ and $\Psi_h(r_h)$ are the radial part of the normalized eigenfunction for the electron and hole, respectively. θ is angle between vectors r and r_h. After eq A11 was integrated analytically with respect to θ, numerical computation was performed for eq A12.

$$E_c = -2(e^2/\epsilon)\int_0^\infty r_h\left[\int_0^{r_h}\{\Psi(r)^2\,\Psi_h(r_h)^2/r_h\}r^2\, dr + \int_{r_h}^\infty \Psi(r)^2\Psi_h(r_h)^2 r\, dr\right] dr_h \quad \text{(A12)}$$

Characterization of the $KrCl_2$ and $XeCl_2$ van der Waals Isomers

Craig R. Bieler, Kevin E. Spence, and Kenneth C. Janda*

Department of Chemistry, University of Pittsburgh, Pittsburgh, Pennsylvania 15260
(Received: October 5, 1990; In Final Form: January 22, 1991)

The observation of van der Waals isomers of $KrCl_2$ and $XeCl_2$ by two-laser pump-probe spectroscopy is reported. Both complexes are found to be T-shaped in the ground electronic state and at least up to $v = 11$ in the B excited electronic state. Analysis of the Cl_2 fragment rotational distributions yields a van der Waals dissociation energy of 236.6 ± 2.0 cm^{-1} (2.84 ± 0.02 kJ/mol) in the ground state for $KrCl_2$ and 286.3 ± 1.1 cm^{-1} (3.44 ± 0.01 kJ/mol) in the ground state for $XeCl_2$. The fragment rotational distributions suggest that the clusters may vibrationally predissociate via an intramolecular vibrational redistribution process, but the large reduced mass of the complexes causes several collisions to occur before complete dissociation. Several other observations are reported which suggest that electronically nonadiabatic relaxation channels are available to the complexes and compete with vibrational predissociation.

Introduction

Since XeF_2 was first synthesized nearly three decades ago, there has been great interest in the reactivity between rare-gas atoms and halogens.[1] Prediction of the bonding that occurs in such systems is not easy. For instance, when xenon and fluorine are mixed together, only a small amount of energy is needed to initiate the formation of XeF_2 in which the dissociation energy per bond is 134 kJ/mol. Enough excitement was generated by this discovery that the existence of chemically bonded HeF_2 was proposed![2] However, the only other rare gas-dihalogen molecule that has been well characterized is KrF_2, which is significantly less stable than XeF_2. Waters and Gray[3] estimated that linear Cl-Xe-Cl would have a potential minimum with each Xe-Cl bond having a dissociation energy of 29.7 kJ/mol. Some time later, Klemperer and co-workers[4,5] hypothesized that the ArClF and KrClF molecules exhibited signs of incipient chemical bonding. Despite these predictions, no other chemically bonded rare gas-dihalogen

(1) Bartlett, N.; Sladky, F. O. In *Comprehensive Inorganic Chemistry*; Pergamon: New York, 1973; Vol. 1, pp 213-330.
(2) Pimentel, G. C.; Spratley, R. D. *J. Am. Chem. Soc.* **1963**, *85*, 826-827.
(3) Waters, J. H.; Gray, H. B. *J. Am. Chem. Soc.* **1963**, *85*, 825-826.
(4) Harris, S. J.; Novick, S. E.; Klemperer, W.; Falconer, W. E. *J. Chem. Phys.* **1974**, *61*, 193-197.
(5) Novick, S. E.; Harris, S. J.; Janda, K. C.; Klemperer, W. *Can. J. Phys.* **1975**, *53*, 2007-2015.

0022-3654/91/2095-5058$02.50/0